Nanostructured Fly Ash–Styrene Butadiene Rubber Hybrid Nanocomposites

K. Thomas Paul,[1] S.K. Pabi,[2] K.K. Chakraborty,[1] G.B. Nando[1]
[1]*Rubber Technology Centre, Indian Institute of Technology, Kharagpur, India 721302*

[2]*Metallurgical and Materials Engineering Department, Indian Institute of Technology, Kharagpur, India 721302*

Hybrid nanocomposites of styrene butadiene rubber (SBR) with nanostructured fly-ash (NFA) were prepared in the laboratory by melt blending technique in an internal mixer. Curatives were added on a laboratory two-roll mill. Curing characteristics as well as physico-mechanical properties of the composites were evaluated. A comparison on SBR composites filled with fresh fly-ash (FFA); carbon black (CB) and precipitated silica (PS) has been reported. In general, SBR-NFA composites exhibit higher state of cure and higher strength properties as compared with HAF black-filled and fresh fly-ash-filled SBR composites at equivalent loadings. This may be attributed to the higher reinforcing ability of NFA. This fact has also been supported by the swelling studies and Kraus' plot. Tear strength and abrasion resistance of the SBR-NFA composites were superior to FFA-filled and precipitated silica-filled vulcanizates, but were inferior to carbon black- filled SBR vulcanizates. The SBR-NFA composites showed lower hardness as compared with both the carbon black-filled and silica-filled composites. Transmission electron microscopy and scanning probe microscopy studies revealed that the NFA particles are well dispersed in the SBR matrix. These results were further supported by fracture surface analysis under the SEM, which revealed the role of NFA in the prevention of fracture propagation. POLYM. COMPOS., 30:1647–1656, 2009. © 2008 Society of Plastics Engineers

INTRODUCTION

Rubber industry is an important resource-based industry in the world [1]. Being a material of low modulus, rubber needs reinforcement for enhancing its strength and performance. A wide range of particulate fillers are used in the rubber industry to improve and modify its physico-mechanical properties. Carbon black is the most important reinforcing filler used so far owing to its superior rubber-filler interactions due to the larger surface area and higher surface activity leading to bound rubber formation, as illustrated by Kraus [2]. The bound rubber formation is believed to enhance the mechanical strength properties of the carbon black filled rubber composites [3]. Second to carbon black is the silica, both precipitated as well as pyrogenic, used as a reinforcing filler under the non-black category also has lower particle size and larger surface area but relatively less surface activity for enhancing technical properties of rubber products. The unique advantages of precipitated silica-reinforced rubber compounds include improvement in tear, flex, abrasion, heat resistance, hardness, modulus, resilience, and rolling resistance [4]. Active functional groups on silica surface, such as hydroxyl and alkoxyl, make this filler more acidic and hydrophilic. This may lead to poor rubber-filler interactions [5]. However, establishment of molecular bridges between the rubber hydrocarbon and silica surface by using bifunctional organosilane coupling agents significantly improves the filler-rubber interactions in silica filled rubber compounds, thus enhancing the physico-mechanical properties of the vulcanizates. Apart from silica, use of other inorganic fillers containing silica, such as clay, black rice-husk ash (BRHA), and white rice-husk ash (WRHA), as a reinforcing or semi reinforcing filler in rubber has been reported in literature [6–8].

Combustion of coal in the thermal power plants generates a huge quantity of fly-ash as a by product, which is a waste causing a threat to the environment. Research is in progress to utilize this huge waste as a resource material for making cement, bricks and tiles, etc. An attractive way to utilize this huge industrial waste in the rubber industry is explained here.

Fly-ash typically contains more than 50% silica by weight and can be potentially used as the partial or full replacement of silica in elastomers. Several researchers have reported the effect of fly-ash as a utility filler in elastomer compositions, but the results, in general, were not encouraging. Some of such literatures are cited here. Hundiwale et al. [9, 10] have compared the effects of var-

Correspondence to: G.B. Nando; e-mail: golokb@rtc.iitkgp.ernet.in
DOI 10.1002/pc.20738
Published online in Wiley InterScience (www.interscience.wiley.com).

ious mineral fillers in natural rubber and SBR composites and suggested that fly-ash can be used as a potential substitute to calcium carbonate. Garde et al. [11] indicated that the mechanical properties of polyisoprene rubber loaded with fly-ash were inferior to those of polyisoprene filled with silica. Many other researchers have reported [12–15] marginal improvement in technical properties with the incorporation of fly-ash as filler by using a suitable coupling agent. Alkadasi et al. [12, 13] reported that the use of silane coupling agent enhances the rubber-filler interactions in fly-ash filled polybutadiene and SBR compounds. Sombatsompop et al. [14] studied the effects of untreated precipitated silica and fly-ash silica as fillers on the technical properties of natural rubber and SBR compounds. They recommended that fly-ash silica could be utilized as filler in natural rubber at concentrations below 30 phr but could not be used in SBR because of property deterioration. Use of silane and titanate coupling agents is likely to improve the mechanical properties of fly-ash filled chloroprene rubber composites [15].

The reasons for the inferior performance of unmodified fly-ash filled rubber vulcanizates has been attributed to the poor filler-rubber interactions because of its very smooth and inert surface. Also the highly crystalline structure and coarse particle size plays a significant role in its incompetence. The present authors [16] have recently reported overcoming these difficulties by preparing nanostructured fly-ash (NFA) by mechanical activation and modifying it to suit as reinforcing filler in rubber. The nanostructured fly-ash has an increased surface area and improved surface activity and reduced crystallinity. The surface smoothness was destroyed and irregularity was introduced, which proved advantageous for the better mechanical interactions with the rubbers. The crystallinity of the fly-ash was found to decrease drastically by mechanical activation process.

The present study is intended for comparing the performance of NFA as a filler with unmodified fly-ash, i.e., fresh fly-ash (FFA), as well as conventional fillers such as carbon black (N 330) and precipitated silica in a noncrystallizable rubber like styrene butadiene rubber. The curing characteristics, mechanical strength and morphological studies have been documented.

EXPERIMENTAL

Materials Used

The fly-ash from the Kolaghat thermal power station, India, was ball milled to nanoscale using a planetary ball mill (Frisch Pulverizette, Germany). The nanostructured fly ash (NFA) obtained has an average particle size of 148 nm and specific surface area of 25.53 m^2/g. Styrene-butadiene rubber, SBR 1502 (Synthetics and Chemicals, India), zinc oxide (Merck, Mumbai, India), *N*-cyclohexyl-2-benzothiazyl sulphenamide (CBS), tetra methyl thiuram disulphide (TMTD), and rubber grade sulphur (Bayer, India) were used in this study. Bis(3-triethoxy silyl propyl) tetrasulphide (TESPT) employed as the coupling agent for siliceous fillers was procured from Birla Tyres, India. Commercial grades of precipitated silica and HAF black (N 330) was used in this study.

TABLE 1. Composition of the mixes.

	FFA composites	NFA composites	CB composites	PS composites
SBR 1502	100	100	100	100
Zinc oxide	5	5	5	5
Stearic acid	2	2	2	2
CBS	1.5	1.5	1.5	1.5
TMTD	0.5	0.5	0.5	0.5
Sulphur	2	2	2	2
FFA	1,2,4,8,16			
NFA		1,2,4,8,16		
Carbon black			1,2,4,8,16	
Precipitated silica				1,2,4,8,16
Si-69	4	4		4

FFA, fresh fly-ash; NFA, nanostructured fly-ash; CB, carbon black; PS, precipitated silica.

Preparation of Rubber Compounds

The mixing of rubber with nanostructured fly-ash and additives were carried out in a Brabender Plasticorder (PLE 330) at a temperature of 100°C and at a rotor speed of 60 rpm. The curatives (sulphur and accelerators) were added into the rubber later on the two roll mill at room temperature, and refined for homogeneity. Semi-efficient vulcanizing system was used in the study with sulfur as the curative, zinc stearate as cure activator and CBS-TMTD as accelerator system as per the composition given in the Table 1. TESPT was used as the coupling agent for fly-ash as well as silica filler, and the dose was kept at 4 phr. TESPT was allowed to wet the fly-ash surface prior to mixing. The paste like mass was incorporated to the rubber before zinc oxide addition. This is to avoid a possible interaction of zinc oxide with TESPT.

Curing Characteristics

The curing characteristics of the rubber compounds at 150°C was determined by an oscillating disc rheometer (Monsanto R100), as per ASTM D 2084 81 and the results was reported in Table 2.

Measurement of Mechanical Properties of Nanocomposites

The mechanical properties of nanostructured fly-ash (NFA) filled SBR composites with various proportions of

 DOI 10.1002/pc

TABLE 2. Comparison of cure characteristics of various fillers.

	NFA		FFA		Carbon black (N 330)		Precipitated silica	
Dosage	M_H (dN m)	T_{90} (min)	M_H (dN m)	T_{90} (min)	M_H (dN m)	T_{90} (min)	M_H (dN m)	T_{90} (min)
0	47	18.29						
1	86	17.49	50	8.86	70	16.75	67	17.75
2	89	17.08	64	14.00	68	14.00	72	17.75
4	91	13.61	66	15.63	72	14.00	75	17.75
8	93	13.71	85	13.75	77	13.50	80	15.25
16	95	13.24	88	14.00	81	13.75	84	14.25

filler were studied and compared with those containing conventional fillers like carbon black (CB) and precipitated silica (PS). Test specimens were molded in an electrically heated hydraulic press at 150°C under a pressure of 45 MPa for the respective optimum cure times predetermined by Monsanto rheometer. Dumb bell specimens were punched out from the molded sheets, and the tensile properties were determined using a Hounsfield 25 KS Universal Testing Machine at a cross head speed of 500 mm/min as per ASTM standard D 412 87. Tear strength of the specimens were determined as per ASTM D 624 86. Hardness of the specimens was measured as per ASTM D 2240 86, using an indentation hardness tester (Shore A Durometer). Abrasion resistances of the specimens were studied in a Du-Pont croydon abrader; the results being expressed as the volume loss per hour. Heat build-up of the specimens was measured using Goodrich flexometer, as per ASTM D 623 83.

Swelling Studies

The volume fraction of rubber in the swollen gel, V_r was determined by equilibrium swelling technique using toluene as the solvent. A known volume of rubber vulcanizates in the form of a round pellet was taken for swelling study in toluene. After attaining equilibrium swelling, its weight was noted and then it was kept for de-swelling at room temperature (30°C) until a weight difference of 0.05 g. Volume fraction of rubber (V_r) in the swollen gel [17] is directly related to the chemical crosslink density, which is calculated by

$$V_r = \frac{(D - FT)\rho_r^{-1}}{(D - FT)\rho_r^{-1} + A_0\rho_s^{-1}}$$

where, D is the de-swollen weight of vulcanizates, F is the weight fraction of the insoluble components of the vulcanizates, T is the initial weight of the sample, ρ_r is the density of the rubber, A_o is the weight of solvent absorbed under equilibrium condition, and ρ_s is the density of the solvent.

Bound Rubber Studies

Bound rubber content was determined by extracting the unbound materials such as ingredients and free rubbers with toluene for seven days and dried for two days at room temperature. Weights of the samples before and after the extraction were measured and the bound rubber contents were calculated using equation [18] given below.

$$R_b(\%) = \frac{(W_{fg} - W_t\phi_f)}{W_t\phi_r} \times 100$$

where R_b is the bound rubber content, W_{fg} is the weight of filler and gel, W_t isthe weight of the sample, Φ_f is the weight fraction of filler in the compound; Φ_r is the weight fraction of rubber in the compound; the values are calculated by

$$\phi_f = m_f/(m_r + m_f)$$

and

$$\phi_r = m_r/(m_r + m_f)$$

where m_f is the weight of the filler in the compound and m_r is the weight of the rubber in the compound.

Microscopic Studies

The tensile fractured surfaces of NFA-filled, FFA-filled, CB-filled, and PS-filled SBR composites were examined under a JEOL JSM 850 scanning electron microscope (SEM). Transmission electron microscope (TEM) studies of the composites was carried out using JEOL 2010 Japan TEM for understanding the dispersion of nanostructured fly-ash in the SBR vulcanizates. Scanning probe microscopic (SPM) images were obtained using an SPM of Nanonics imaging limited, Israel.

RESULTS AND DISCUSSIONS

Cure Characteristics

The curing characteristics of the rubber compounds are essential as it predicts the behavior of the compounds during processing, scorch safety, stability, and the physicomechanical properties of the final vulcanizates. The curing characteristics of all the mixes are summarized in Table 2. The maximum torque value (M_H), which corresponds

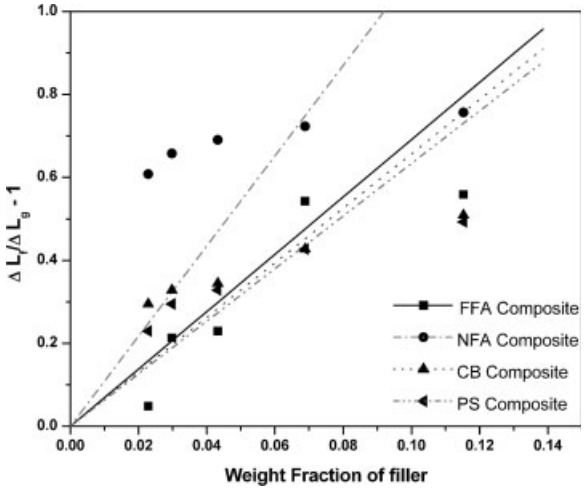

FIG. 1. Plots according to Westlinning–Wolf equation for composites with various fillers.

to the state of cure of the vulcanizate has a direct relationship with the modulus of the vulcanizate. Optimum cure time (T_{90}), which is the time to develop 90% of full torque or time for torque to increase to $T_{90} = 0.9(M_H - M_L) + M_L$ [19]. M_H is the highest torque attained during specified period of time and M_L is the minimum torque obtained during cure tests carried out in oscillating disc rheometer (ODR). T_{90} reflects the formation of maximum crosslink density responsible for the highest possible physico-mechanical properties.

As the filler dosage increased, the M_H value increased. This is expected since rubber matrix gets reinforced till a certain dose of the filler beyond which no more increase is observed due to saturation and dilution effect. M_H of the NFA filled SBR compounds was higher in comparison with those of compounds filled with fresh fly-ash (FFA), carbon black (CB), and precipitated silica (PS). About 16 phr of NFA lead to a torque of 95 N m, which was higher than 88 N m, that of FFA, 81 N m, that of carbon black and 84 N m, that of precipitated silica. The optimum cure time, however, showed no significant difference with respect to the type of filler used, although the cure time decreased with increasing dosage of filler regardless of its type.

The increase in the maximum torque value is attributed to the enhanced filler- polymer (rubber) interactions [20]. This behavior is further supported by the plots shown in Fig. 1 according to Westlinning–Wolff's equation [21]

$$\alpha_F = \frac{\left(\frac{\Delta L_f}{\Delta L_g} - 1\right)}{w}$$

where, ΔL_f and ΔL_g are the Rheometric torque differences between maximum and minimum torque values for filled and gum compounds, w is the weight fraction of filler in the polymer. α_f, obtained from the slope of the plot and is known to represent the filler activity. According to Fig. 1, α_f value for NFA-SBR composites was 10.87 and those for carbon black filled and precipitated silica filled composites were 6.57 and 6.33, respectively. The higher α_f value of NFA-SBR composites are due to the enhanced filler-rubber interactions.

Mechanical Properties

Tensile properties of SBR vulcanizates filled with fresh fly-ash (FFA), nanostructured fly-ash (NFA), carbon black and precipitated silica with respect to increase in loading of the filler are shown in Figs. 2–4. Figure 2 shows the tensile strength of the SBR vulcanizates with increase in dose of the fillers varying from 1 to 16 phr. It is observed that the tensile strength improves with increase in the filler content in all the cases. The gum vulcanizate showed a lower tensile strength of 1.98 MPa. When NFA is incorporated into SBR, the tensile strength increased continually with increase in the NFA level. At 16 phr, it attained a value of 7.44 MPa with a record improvement of 270%. On the other hand, incorporation of other fillers such as carbon black, silica and fresh fly-ash although improved the tensile strength, but they did not reach the same level as observed in the case of NFA filled SBR vulcanizate. FFA-SBR composites imparted a value of 3.67 MPa, i.e., an enhancement of only 70% at a loading of 16 parts. HAF black recorded a tensile strength increase up to 171% at 16 phr loading, whereas the precipitated silica recorded an improvement in tensile strength of 181%. Thus NFA stands far ahead of the precipitated silica and carbon black (HAF) in the reinforcement ladder. This can be attributed to two factors. First, the fly-ash has a major proportion of silica in it. Majority of this crystalline silica was converted into amorphous nano-silica in the NFA due to mechanical break down. Secondly, it contains alumina, which is present in the form of aluminium silicate. During mechano-chemical break down, it possibly converted into nano-clay (hydrated aluminium silicate), thus contributing

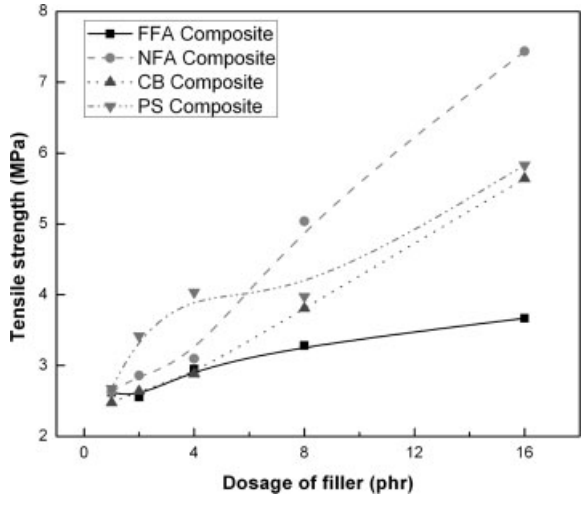

FIG. 2. Variation of tensile strength with filler dosage.

DOI 10.1002/pc

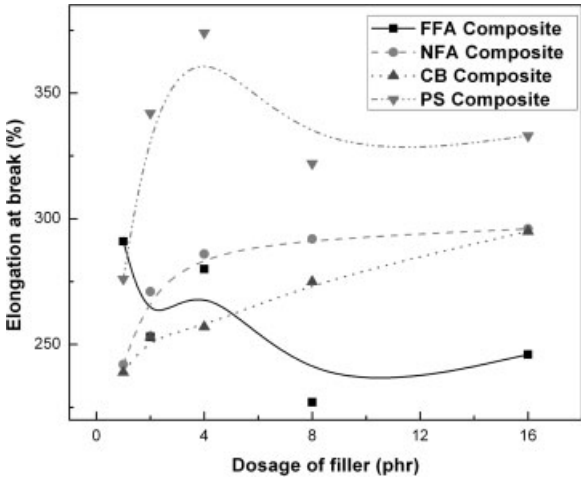

FIG. 3. Variation of elongation at break with filler dosage.

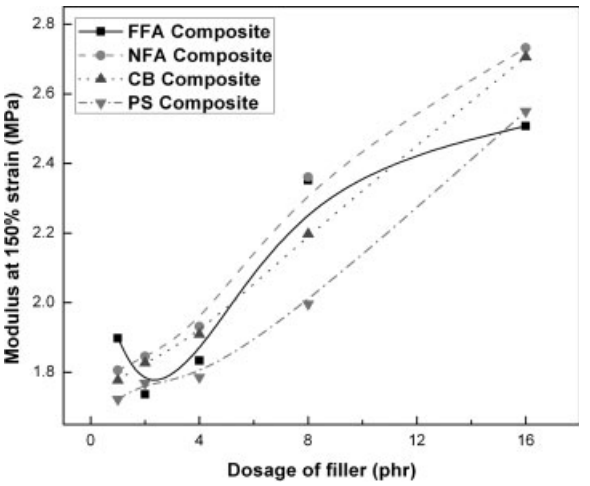

FIG. 4. Variation of modulus at 150% with filler dosage.

to the reinforcement phenomenon. Further studies are in progress to understand this clay like structure formed due to mechanical break down.

Figure 3 describes the variation of elongation at break with increase in the filler loading with all the four types of fillers in SBR. The elongation at break first increased with increasing the filler content then it reached a plateau or marginally reduced in the case of NFA, carbon black and precipitated silica except in the case of fresh fly-ash which continuously increased. Addition of NFA did not make the vulcanizate rigid as evidenced by its higher elongation at break even up to 16 phr loading of NFA. Modulus at 150% shown in Fig. 4 follows the same trend as of tensile strength, i.e., it increases with the filler content. The maximum enhancement in modulus is shown by NFA at 16 phr loading.

The improvement in tensile properties provides direct evidence of the enhanced polymer-filler interactions. Initially the fresh fly-ash (FFA) has a spherical shape, with smooth surface finish and with low surface activity. The particle size is also large, i.e., in the range of micrometers (60–100 μm). When converted into nanostructured fly-ash, the particle size reduced from micron size to nanoscale, the spherical shape got broken down to irregular shapes and the surface smoothness also destroyed resulting in an effective increase in surface area. These structural factors contributed to more interactions with the rubber matrix, when it is incorporated into a rubber. The enhanced surface activity is also evident from the FTIR studies reported recently by the authors [16]. The large interfacial area of NFA seems to play an important role in the improvement of properties, since high strength of the composites was obtained even at lower levels of fillers, thus resulting in composites with high strength to weight ratio.

Figure 5 shows the abrasion loss of the SBR vulcanizates with filler loadings of up to 16 phr. A loss of 0.16 cm^3/h was observed for composites with 1 phr of NFA. Increasing the dosage of NFA to 16 phr, a volume loss of 1.02 cm^3/h has been observed. However, this increase in volume loss was more up to 4 phr of NFA; thereafter the loss remained insignificant with little change in filler level up to 16 phr. In comparison with the other siliceous fillers like precipitated silica, the abrasion loss was less in the NFA-SBR nanocomposites, whereas in the case of precipitated silica filled composites, the loss continued to increase with increasing the loading. Carbon black, on the other hand, was found to be very efficient in this regard. It imparted higher abrasion resistance to the composites, as is evident from continuous decrease in abrasion loss with increasing carbon black dosage. This effect has been attributed to enhanced fraction of bound rubber with the carbon black filled SBR vulcanizates.

Figure 6 displays a comparison of the tear strength property of the composites containing four different fillers. The tear strength increased very rapidly with an increase in the dosage of the fillers. FFA showed a slow increase whereas NFA, carbon black and precipitated silica incorporation rapidly enhanced the tear strength of the SBR vulcanizates. Carbon black showed the highest

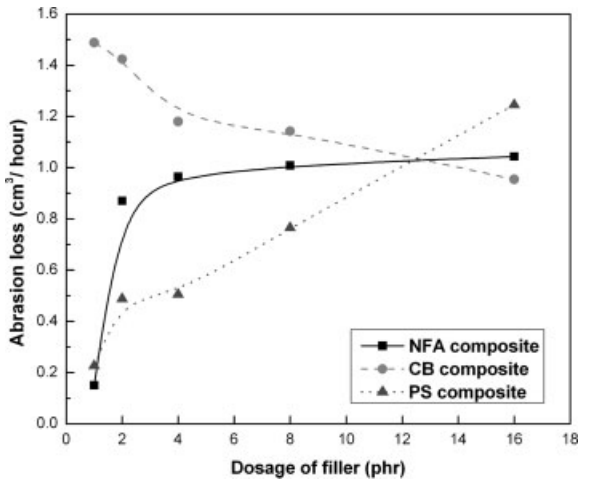

FIG. 5. Variation of abrasion loss with filler dosage.

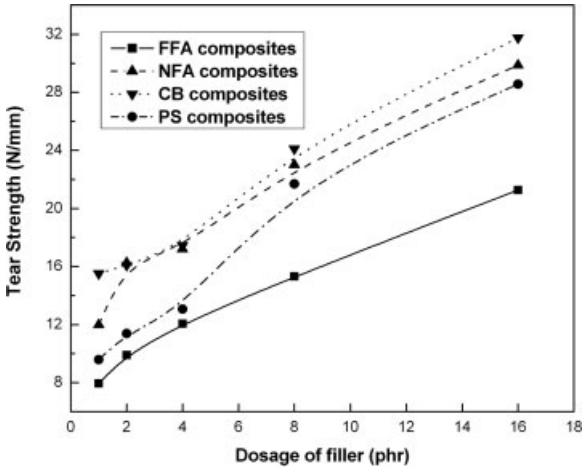

FIG. 6. Variation of tear strength with filler dosage.

tear strength followed by NFA, which is followed by precipitated silica. It is interesting to observe that 1 phr of NFA and carbon black enhanced the tear strength of SBR vulcanizates to 11.97 and 15.5 N/mm, respectively whereas 16 phr of NFA and carbon black further enhanced the tear strength to 28 and 32 N/mm, respectively. This phenomenon can be explained on the basis of filler-rubber interaction and bound rubber formation.

Figure 7 shows the hardness of the composites by varying the filler loading from 1 to 16 phr. There was no significant change in Shore A hardness values on increasing the filler dosage except for carbon black filled composites which showed a sharp increase beyond 8 phr of loading. NFA showed a marginal increase up to 4 phr beyond which it remained constant till 16 phr of loading. This is in contrast to the change in tensile modulus which increased steadily with loading of NFA.

The increased filler-rubber interaction reflected in Goodrich heat build up results which are illustrated in the Fig. 8. NFA-filled SBR composite having the filler level

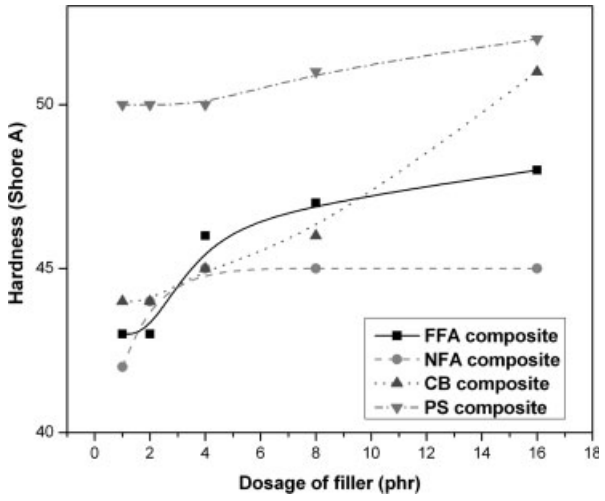

FIG. 7. Variation of hardness with filler dosage.

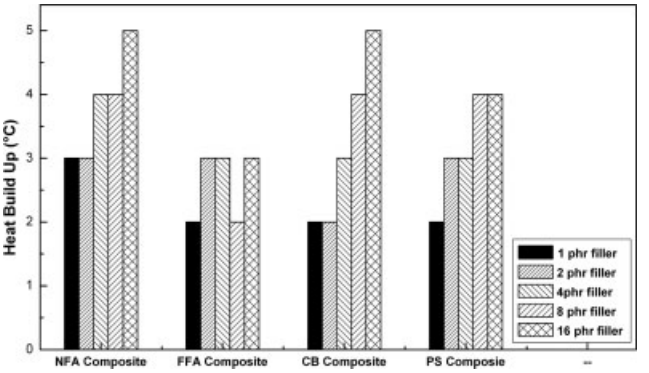

FIG. 8. Variation of heat build up with filler dosage.

of 16 phr showed a higher heat build up of 5°C which levels with the carbon black filled composite at the same filler loading. The heat build up value of FFA filled composite is 3°C at 16 phr, which is the lowest value compared with all other fillers under study. The precipitated silica (PS)-SBR composite showed a heat build up of 4°C at a filler dosage of 16 phr.

The increase in specific gravity with the dosage of various fillers is summarized in Fig. 9. It is interesting to observe that, even though NFA is siliceous filler, the increase in specific gravity is not so significant. This filler lead to formation of vulcanized products with high strength to weight ratio, as in the case of carbon black. The mechanical property studies conclude that the NFA can be considered as a promising reinforcing filler, with properties analogous with carbon black filler in many respects.

Swelling Studies

The volume fraction of rubber in the swollen vulcanizates (V_r) has a direct relationship with the crosslink density. The V_r value of the vulcanizates is an estimate of the reinforcing ability of the filler. The V_r is determined by

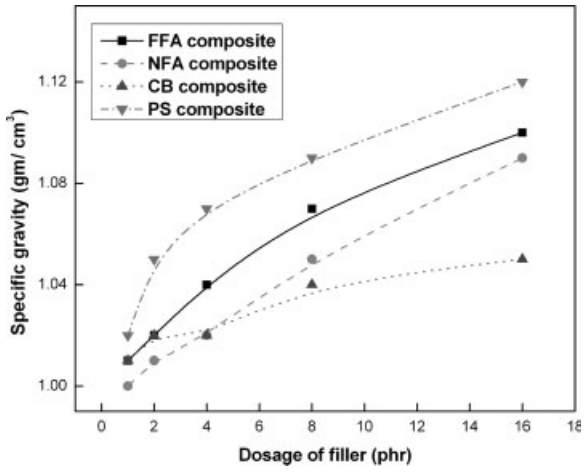

FIG. 9. Variation of specific gravity with filler dosage.

DOI 10.1002/pc

TABLE 3. Volume fractions of rubber in swollen vulcanizates.

Filler loading	FFA	NFA	Carbon black	Precipitated silica
1	0.337	0.364	0.341	0.336
2	0.343	0.376	0.346	0.338
4	0.344	0.388	0.366	0.358
8	0.355	0.399	0.385	0.364
16	0.344	0.426	0.383	0.379

swelling method and is presented in the Table 3. As expected, the volume fraction of rubber increased with the increase in filler content for all the fillers. Also the highest V_r value obtained at 16 phr of NFA loading is an evidence of the reinforcing ability of NFA in SBR matrix, which supports the tensile strength results reported in the Fig. 2. A similar trend was also observed with carbon black as well as precipitated silica filler as shown in Table 3.

Figure 10 shows the plots according to Cunnen–Russel equation [22]:

$$\frac{V_{r0}}{V_{rf}} = ae^{-z} + b$$

where, V_{r0} and V_{rf} are the volume fraction of rubber in the gum and filled vulcanizates, respectively. The ratio of V_{r0} to V_{rf} is a measure of rubber-filler interaction in filled system. z is the weight fraction of filler in composite, a and b are two constants, which are dependant on the filler activity. The values of a and b calculated from the plots are given in Table 4. Higher value of a and lower value of b indicate strong rubber-filler interaction. Both the requirements are favorable in the case of NFA-SBR nanocomposites as compared with the other filler systems in the present study.

Figure 11 shows the plot of V_{r0}/V_{rf} against $\theta/(1-\theta)$ according to Kraus equation [23]:

$$\frac{V_{r0}}{V_{rf}} = 1 - \frac{m\theta}{(1-\theta)}$$

where,

$$m = 3C\left(1 - V_{r0}^{1/3}\right) + V_{r0} - 1$$

here, C is the characteristic constant for filler, which is independent of solvent. θ is the volume fraction of filler in the vulcanizate, m represents the polymer-filler interaction parameter obtained from the slope of the plot of V_{r0}/V_{rf} against $\theta/(1-\theta)$. Highest value of m observed for NFA-SBR nanocomposites is attributable to its higher reinforcing ability. The interaction parameter for NFA was found to be 0.653 as compared with 0.569 for carbon black and 0.588 for precipitated silica. Fresh fly-ash filled vulcanizates yielded the lowest value of 0.088 evidencing its lack of reinforcement in SBR vulcanizates.

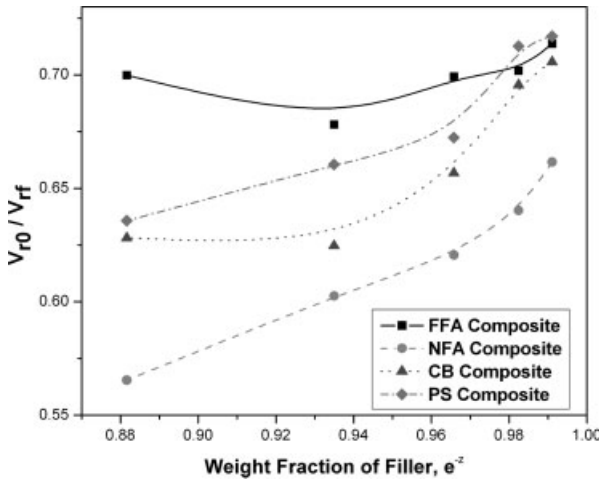

FIG. 10. Plots according to Cunnen–Russel equation for composites for various fillers.

The reinforcing phenomenon between the filler and a rubber may be explained by two distinct mechanisms. One is the increase in stiffness of the rubber matrix imparted by the active filler. This creates a hydrodynamic effect, which in turn reinforces the rubber matrix. This effect has been mathematically quantified [24] by Guth and Gold equation and is given by

$$G = G_o(1 + 2.5\varphi + 14.1\varphi^2) = G_0X$$

where G_0 is the modulus of the matrix and ϕ is the volume fraction of the filler. This effect is expected to be playing a major role in rubber compounds filled with rigid particulate fillers.

Other contribution towards the reinforcement is from the molecular interactions between rubber and the filler. These interactions lead to an increase in the effective degree of crosslinking, which in turn enhances the mechanical properties of the vulcanizates. The improvement of filler-rubber interactions with the incorporation of NFA has been established from the cure characteristics, mechanical properties and swelling studies as discussed above. In all these studies, NFA reinforced composites excel over carbon black, precipitated silica and fresh fly-ash filled composites. The reduced particle size, increased surface area, enhanced surface roughness and creation of active –OH group on filler surface are instrumental in enhancing the filler- rubber interactions in NFA filled nanocomposites.

Bound Rubber Studies

The bound rubber content of the composites has been studied and reported in the Fig. 12. As the dosage increased, the bound rubber content also increased in the case of all fillers in this study. NFA-SBR composites showed higher bound rubber content as compared with FFA-SBR composites or precipitated silica filled compo-

TABLE 4. Characteristic constants according to Cunnen–Russel equation.

	a	B
FFA Composites	0.0122	0.5829
NFA Composites	0.8083	−0.1507
CB Composites	0.7120	−0.0227
PS Composites	0.7330	−0.0176

sites. Carbon black filled composites show the bound rubber values comparable with those of NFA-SBR composites. The bound rubber study also underlines the efficiency of NFA in interacting with the rubber matrix. The bound rubber content of FFA-SBR composites were inferior to all the other systems studied. The size reduction of fly-ash by high energy milling not only produced nanostructured materials, but it also generated surface active groups conducive for better bonding.

Morphological Studies

Figure 13A–D displays the SEM photomicrographs of the tensile fractured surfaces of SBR composites with various fillers at 16 phr loading.

Figure 13A shows the SEM photomicrograph of FFA-SBR composite. The inferior performance of FFA-SBR composite was attributed to the poor rubber-filler interaction. This fact is visualized in SEM studies. The surface of the FFA is totally unaffected by the rubber and the fractured surface show delaminating tendency at the filler-rubber interface. The large particle size also plays its role in weakening the composite. Figure 13B shows the tensile fractographs of CB-SBR composite with 16 phr. As expected, the carbon black particles are found to be wrapped up in the rubber matrix. This supports the bound rubber theory of carbon black reinforcement; the formation of which imparts all desirable properties to the rubber matrix. Figure 13C shows the SEM images of PS-SBR

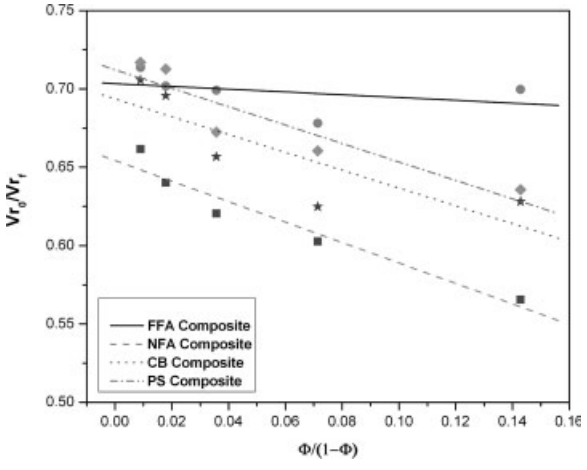

FIG. 11. Kraus' plot for various composites with various fillers.

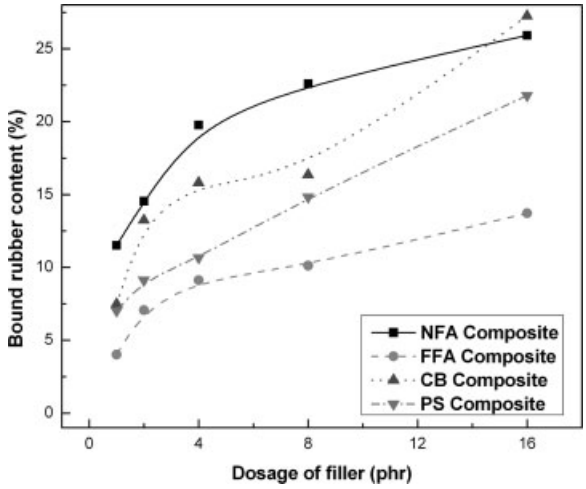

FIG. 12. Variation of bound rubber content with filler dosage.

composite at a filler level of 16 phr. Even though precipitated silica particles have particle size in nanometer range, the surface of the silica is so active that it prefers strong filler networks rather than filler-rubber interactions. The formation of filler network reduces the effective surface area for the interaction with the rubber and the filler exist in the rubber matrix as agglomerated domains rather than distributed particles.

Figure 13D shows the SEM image of NFA-SBR hybrid nanocomposite. The SEM image shows uniform distribution of NFA particles in the SBR matrix. NFA as it produced by high energy milling has a highly active surface, which has the tendency to agglomerate. During mixing with rubber, these aggregates may break down and get wet in the SBR matrix due to the surface active groups of the as-milled filler, which is conducive for good interaction with the surrounding rubber matrix. This can lead to occlusion of the NFA in the SBR matrix forming structures, similar to the bound rubber in carbon black filled elastomers.

The dispersion of NFA in SBR matrix may be more clearly visualized from the TEM studies. Figure 14 shows the TEM image of NFA-SBR composites. Here the nano-sized particles are uniformly dispersed. This increases the effective filler-rubber interface and supports the fact that, filler-rubber interactions are more pronounced compared with filler-filler interactions in NFA-SBR composites, and there is less chances of forming filler network, which normally occurs in the silica filled composites.

The scanning probe microscopic (SPM) height image of 16 phr filled NFA-SBR composite is shown in Fig. 15. A scan area of 1 μm $\times$ 1 μm was chosen for the study. The lighter shade in the image corresponds to the harder parts, which is the dispersed NFA particles in the SBR matrix (darker shade). The image describes that the NFA particles of around 100 nm in size are dispersed uniformly in the rubber matrix and there are no agglomerations. Also the rubber matrix is strongly adhered to the NFA surface which supports the adequate filler-rubber

DOI 10.1002/pc

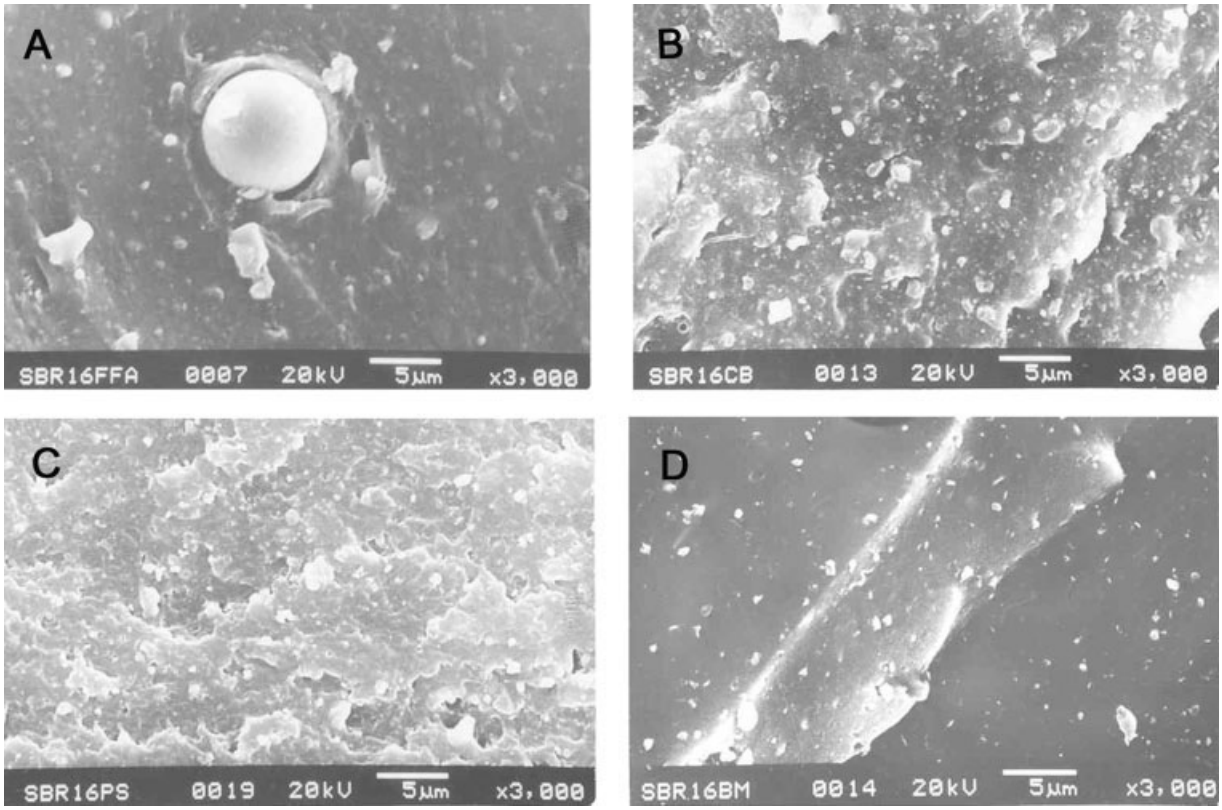

FIG. 13. SEM images of SBR composite with various filler at a dosage of 16 phr. (A) FFA-SBR composite at 3,000 times magnification, (B) CB-SBR composites at 3,000 times magnification, (C) PS-SBR composites at 3,000 times magnification, and (D) NFA-SBR composites at 3,000 times magnification.

interactions to form bound rubber-like fractions and that may promote the high-end performance of rubber compound in industrial applications.

CONCLUSIONS

SBR-NFA hybrid nanocomposites show higher value of maximum torque, which is an indication of the higher state of cure compared with fresh fly-ash filled, carbon black filled and precipitated silica filled SBR composites. SBR-NFA composites show apparently higher crosslink density and higher polymer-filler interaction parameter as evident from the swelling studies. The superior filler-rubber interactions in the SBR-NFA hybrid composites affected in the enhancement of mechanical properties. These composites displayed considerable increase in tensile properties and tear strength compared with those of the gum stock as well as composites filled by conventional fillers even for loading of only 16 phr. The tensile

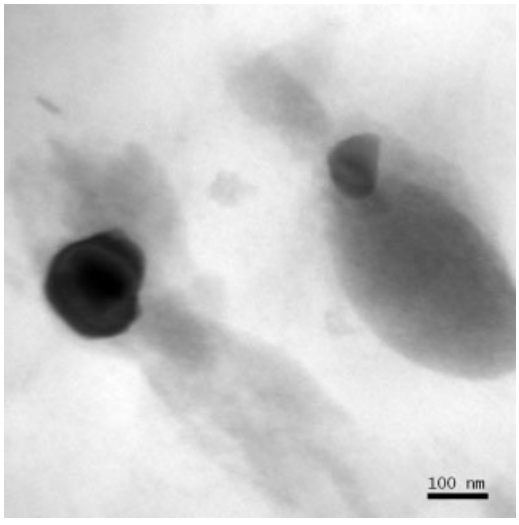

FIG. 14. TEM image of nanostructured fly-ash filled SBR composite.

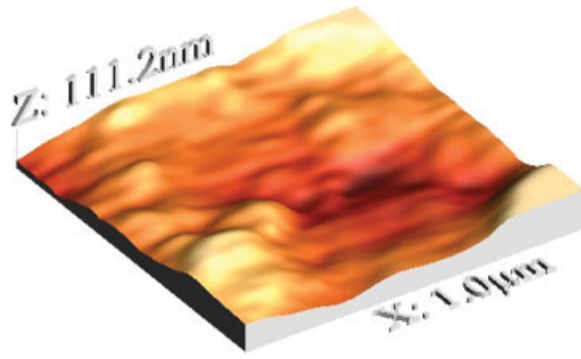

FIG. 15. SPM image of nanostructured fly ash filled SBR composite (16 phr). [Color figure can be viewed in the online issue, which is available at www.interscience.wiley.com.]

fractographs studied under SEM evidenced improved wetting, good rubber-filler interactions and good dispersion of NFA in the matrix. TEM and SPM studies revealed that nanosized particles of NFA were more or less uniformly dispersed in the rubber matrix with low levels of agglomeration.

REFERENCES

1. Asian Rubber Handbook and Directory Dhanam, Kochi, India, 25 (2003).
2. G. Kraus, *Reinforcement of Elastomers*, Wiley, New York (1965).
3. S. Ono, Y. Kiuchi, J. Sawanobori, and M. Ito, *Polym. Int*., **48**, 1035 (1999).
4. L.K. Mark and J.L. Koenig, *Rubber Chem. Technol*., **71**(**2**), 300 (1998).
5. A. Ansarifar, L. Wang, R.J. Ellis, and S.P. Kirtley, *Rubber Chem. Technol*., **79**(**1**), 39 (2006).
6. P.K. Pal, S.N. Chakravarthy, and S.K. De, *J. Appl. Polym. Sci*., **28**, 659 (1983).
7. L. Sereda, L.L. Visconte, R.C.B. Nunes, C.R.G. Furtado, and E. Riande, *J. Appl. Polym. Sci*., **90**, 421 (2003).
8. H.M. de Costa, L.L. Visconte, R.C.B. Nunes, and C.R.G. Furtado, *J. Appl. Polym. Sci*., **87**, 1405 (2003).
9. D.G. Hundiwale, U.R. Kapadi, M.C. Desai, A.G. Patil, and S.H. Bidkar, *J. Sci. Ind. Res.* (*India*), **62**(**8**), 796 (2003).
10. D.G. Hundiwale, U.R. Kapadi, M.C. Desai, and S.H. Bidkar, *J. Appl. Polym. Sci*., **85**, 995 (2002).
11. K. Garde, W. McGill, and C.D. Wooland, *Plast. Rubber Compos*., **28**, 1 (1999).
12. A.N.A. Nabil, D.G. Hundiwale, and U.R. Kapadi, *J. Appl. Polym. Sci*., **91**(**2**), 1322 (2004).
13. A.N.A. Nabil, D.S. Bhimrao, U.R. Kapadi, and D.G. Hundiwale, *J. Sci. Ind. Res. (India)*, **63**(**3**), 287 (2004).
14. N. Sombatsompop, S. Thongsang, T. Markpin, and E. Wimolmala, *J. Appl. Polym. Sci*., **93**(**5**), 2119 (2004).
15. N. Alkadasi, D. Hundiwale, U. Kapadi, and B. Sarwade, *Gummi. Fasern. Kunststoffe*., **57**(**9**), 595 (2004).
16. K.T. Paul, S.K. Satpathy, I. Manna, K.K. Chakraborty, and G.B. Nando, *Nanoscale Res. Lett*., **2**, 397 (2007).
17. A.R.R. Menon, A.I. Aigbodion, C.K.S. Pillai, N.M. Mathew, and S.S. Bhagwan, *Eur. Polym. J*., **38**, 163 (2002).
18. S.S. Choi, *Polym. Test*., **21**, 201 (2002).
19. R.P. Brown, Guide to Rubber and Plastics Test Equipment, Shawbury, England, 53 (1979).
20. S. Debnath, S.K. De, and D. Khastgir, *J. Appl. Polym. Sci*., **37**, 1449 (1989).
21. H. Westlinning and S. Wolff, *Kautsch. Gummi. Kunstst*., **19**, 470 (1966).
22. J.I. Cunnen and R.M. Russel, *Rubber Chem. Technol*., **43**, 1215 (1970).
23. G. Kraus, *J. Appl. Polym. Sci*., **7**, 861 (1963).
24. L. Bokobza and O. Rapoport, *J. Appl. Polym. Sci*., **85**, 2301 (2002).

 DOI 10.1002/pc